Simulation of femtosecond pulse in a Kerr-lens mode-locked Ti:sapphire laser

E.Nomin-Erdene*, D.Unurbileg, P.Munkhbaatar, Ts.Baatarchuluun, Ts.Khos-Ochir, G.Munkhbayar, N.Tuvjargal, G.Erdene-Ochir, J.Davaasambuu

Laser Research Center, School of Arts and Sciences, National University of Mongolia, 14201, Ulaanbaatar, Mongolia

The Kerr-lens mode-locking (KLM) is known as a suitable method for generation of femtosecond pulses and mode-locked Ti:sapphire laser is now widely used sources of stable, energetic femtosecond pulses. We will present the simulation of KLM in Ti:sapphire laser cavities with a folded-cavity four-mirror by applying the ABCD ray-tracing technique for a Gaussian beam. Simulations will be performed for an asymmetric resonator design. Based on the numerical analysis, we will find the optimum design parameters (slit position, gain cavity spacing, gain medium position) for KLM.

Keywords: Self-focusing, Kerr lensing, Misalignment sensitivity.

I. INTRODUCTION

The Kerr-lens mode-locking (KLM) based on the lens-effect induced in suitable material by a Kerr nonlinearity is straight forward method to generate pulses as short as few femtosecond laser pulses [1]. When a beam propagates through a medium which a refractive index linearly varies with the intensity (Kerr nonlinearity), the well-known optical phenomenon that a self-focusing effect is observed [2]. The self-focusing effect of an intense pulses is successfully exploited in the mode-locking [3]. The optical Kerr effect is responsible for the intensity dependent refractive index change which causes the lensing in the gain medium. When a suitable aperture is located inside the cavity where the intense pulses beam profile is narrowed by the Kerr-lens effect, the continuous-wave (CW) radiation propagation losses are higher than the intense pulse propagation losses [4]. The combination of the Kerr-lens and aperture acts as a fast saturable absorber, then a fast passive gain modulation is obtained [5]. The intensity fluctuations in laser start-up are not intense enough to induces Kerr lensing [6,7], thus acousto-optic modulation, additive pulse mode-locking, impulsive starting i.e [8-17] are required before the KLM. The self-starting KLM is achieved by using a highly nonlinear Kerr medium in the folded cavity.

In this paper we simulate the influence of the Kerr lensing on the beam propagation in a folded-cavity four-mirror resonator by applying the ABCD ray-tracing technique for a Gaussian beam. With a split-step method that dividing the Ti:sapphire crystal to many thin lens-like slices [18] the intensity dependent Kerr-lens effect of the Brewster-plate shaped active medium is described. We introduce the optimum design parameters and discuss the modifications of the beam spot size and radius of curvature in the nonlinear Kerr medium, where the refractive index increases with intensity.

II. BEAM PROPAGATION IN THE RESONATOR

The folded-cavity four-mirror resonator, shown in Fig.1 is used for Ti:sapphire lasers. Parameters l_{12}, l_{23}, l_{34} are lengths of the three arms and R_2, R_3 are curvature radii of M_2 and M_3 mirrors. The beam propagation inside the cavity is expressed by the ABCD round-trip matrices. Due to the astigmatic effect the beam propagation behaviour is different in the tangential *xz* plane and in the sagittal *yz* plane [19].

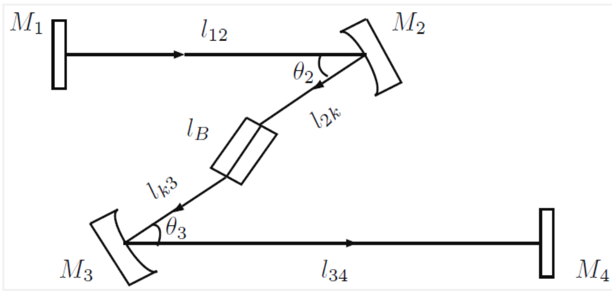

Figure.1 The folded-cavity four-mirror resonator with the Brewster-plate shaped active medium.

The tangential and sagittal rays focus at different positions (astigmatism). This cavity astigmatism is

* Electronic address: nominerdene@num.edu.mn

compensated by the Brewster plate at a certain tilting angle. Without the Kerr lensing the Brewster plate behaves linearly, i.e. ($n_2=0$) [3]. In the case with Kerr lensing the intensity dependence of the refractive index is taken into account in the beam propagation through the gain medium.

For one round trip through the resonator the total ABCD matrix which is the multiplication of all the matrices of the elements is given by

$$M_t = \begin{pmatrix} A_t & B_t \\ C_t & D_t \end{pmatrix} = \prod_i M_i = \prod_i \begin{pmatrix} A_t & B_t \\ C_t & D_t \end{pmatrix} = M_1 M_{12} M_2 M_{2k} M_k M_{k3} M_3 M_{34} M_4 M_{34} M_3 M_{k3} M_k M_{2k} M_2 M_{12}$$

The optical elements in the resonator are listed in Table I. To be a stable resonator, a stability condition, $|A_t + D_t| \le 2$ [20] is required which gives the allowed regions of mirror separation $l_{23} = l_{2k} + l_B + l_{k3}$ for stable laser operation. In this stability region the resonator misalignment sensitivity parameter is determined by $|1/C_t|$ where small value of $|1/C_t|$ implies lower sensitivity of the resonator [5].

Using the ABCD matrices one can calculate the fundamental Gaussian TEM_{00} mode of the cavity for CW operation inside the stability zones of the resonator. The Gaussian mode is represented by the complex beam parameter as

$$\frac{1}{q(z)} = \frac{1}{R(z)} - i\frac{\lambda_L}{\pi w^2(z)} \tag{1}$$

where $R(z)$ and $w(z)$ are the wavefront curvature and the spot size at position z, λ_L is the wavelength. The beam diameter and spot size are related by $\Delta d = [2\ln 2]^{1/2} w$. The beam parameter $q(z)$ for the propagation direction z from z_1 to z_2 is given by

$$q(z_2) = \frac{A_{12} q(z_1) + B_{12}}{C_{12} q(z_1) + D_{12}} \tag{2}$$

The incident beam has the same curvature as mirrors. In our resonator the input mirror M_1 at $z = 0$ is plane, with the radius $R_1(0) = \infty$. Then, the beam parameter for one round trip on this mirror is found as

$$q[0] = i\pi w^2(0)/\lambda_L = [A_t q(0) + B_t]/[C_t q(0) + D_t]$$

Without the Kerr lensing the ABCD matrix components in the equation are constant, thus this quadratic equation can be solved for $q(0)$ and $w(0)$. Considering the Kerr-lens effect, the ABCD matrix components depend on the beam spot size w [3]. To start the ray tracing in the resonator an arbitrary beam parameter is chosen and the calculation is repeated until the real part of the beam parameter $q_{m+1}(0)$ and $q_m(0)$ at the M_1 mirror equals to zero for one round trip.

$$q_{m+1}(0) = \frac{i\pi w_{m+1}^2(0)}{\lambda_L} = \frac{[A_t q_m(0) + B_t]}{[C_t q_m(0) + D_t]} \tag{3}$$

The intensity changes inside the Kerr lens medium is achieved by dividing the crystal to many thin lens-like slices ($l_B \rightarrow 0$) and the beam propagation through each slices is calculated by using the Kerr-lens ABCD matrices given in Table.I with a constant intensity I_{0L}. The solution depends on the crystal position [21].

Table I. ABCD matrices

Optical element	Matrix
Mirror	
Normal incidence	$\begin{pmatrix} 1 & 0 \\ -2/R & 1 \end{pmatrix}$ M_1, M_4
Tilted, sagittal plane	$\begin{pmatrix} 1 & 0 \\ (-2\cos\vartheta)/R & 1 \end{pmatrix}$ M_2, M_3
Tangential plane	$\begin{pmatrix} 1 & 0 \\ -2/(R\cos\vartheta) & 1 \end{pmatrix}$ M_2, M_3
Propagation in space	$\begin{pmatrix} 1 & l \\ 0 & 1 \end{pmatrix}$ $M_{12}, M_{2k}, M_{k3}, M_{34}$
Plate	
Normal incidence	$\begin{pmatrix} 1 & l/n_L \\ 0 & 1 \end{pmatrix}$
Brewster tilted, sagittal plane	$\begin{pmatrix} 1 & l_B/n_L \\ 0 & 1 \end{pmatrix}$ M_k
Tangential plane	$\begin{pmatrix} 1 & l_B/n_L^3 \\ 0 & 1 \end{pmatrix}$ M_k
Kerr-lens plate (tangential thickness l_B)	
Normal incidence	$\begin{pmatrix} \cos(\gamma l) & (l/\tilde{n}\gamma)\sin(\gamma l) \\ -\tilde{n}\gamma\sin(\gamma l) & \cos(\gamma l) \end{pmatrix}$

Tilted to Brewster angle Sagittal plane

$$\begin{pmatrix} \cos(\gamma_s l_B) & (l/\tilde{n}_B\gamma_s)\sin(\gamma_s l_B) \\ -\tilde{n}_B\gamma_s\sin(\gamma_s l_B) & \cos(\gamma_s l_B) \end{pmatrix} \quad M_k$$

Tangential plane

$$\begin{pmatrix} \cos(\gamma_t l_B) & (l/\tilde{n}_B\gamma_t n_L^2)\sin(\gamma_t l_B) \\ -\tilde{n}_B\gamma_t\sin(\gamma_t l_B) & \cos(\gamma_t l_B) \end{pmatrix} \quad M_k$$

Table II. Resonator parameters (λ_L=800nm) [24].

Parameter	Value
Mirror curvatures (mm)	
R_1	∞
R_2	50
R_3	50
R_4	∞
Mirror tilting angles (deg)	
θ_1	0
θ_2	15.22
θ_3	15.22
θ_4	0
Total resonator length (m)	
l_t	1.05
Mirror separators (cm)	
l_{12}	30
$l_{23}=l_{2k}+l_B+l_{3k}$	varied around 5
l_{34} l_t-l_{12}-l_{23}	
Intracavity plate (Brewster-cut Ti:sapphire crystal)	
n_L	1.76
n_2	$1.6\times10^{-22}m^2V^{-2}$ [74]
l_B	2 mm
l_{2k}	varied around $l_{23}/2$

Changing the position of the crystal along the beam affects the mode intensity in the crystal. The optical Kerr effect is a third-order nonlinear process in which the refractive index of the material is intensity dependent [22]. At sufficiently high intensity, the refractive index of the medium will be influenced to a readily observable extent by the field intensity. The Kerr medium is described by the intensity dependent refractive index *n* that is given [1] by

$$n = n_L + \frac{1}{2}n_2E_{0L}^2 = n_L + \gamma_2 I_L = n_L + \frac{n_2}{n_L c_0\varepsilon_0}I_L \tag{4}$$

where n_2 and γ_2 are the nonlinear refractive index and nonlinear coefficient of medium. E_{0L}^2 is the electric field amplitude, $I_L = (n_L c_0\varepsilon_0/2)E_{0L}^2$ is the light intensity c_0 being the light velocity in vacuum and ε_0 the electric permitivity of vacuum).

The Gaussian beam intensity is approximated by a Taylor expansion as

$$I_L = I_{0L}\exp[-2(r/w)^2] \approx I_{0L}[1-2(r/w)^2] \tag{5}$$

then, the (4) equation becomes parabolic [23].

$$\begin{aligned} n &= n_L + \frac{n_2 I_{0L}}{n_L c_0\varepsilon_0}[1-2(r/w)^2] \\ &= (n_L + \frac{n_2 I_{0L}}{n_L c_0\varepsilon_0})(1-\frac{2n_2 I_{0L}}{n_L c_0\varepsilon_0(n_L+\frac{n_2 I_{0L}}{n_L c_0\varepsilon_0})w^2}r^2) \\ &= \tilde{n}(1-\frac{1}{2}\gamma^2 r^2) \end{aligned} \tag{6}$$

where $\tilde{n} = n_L + \frac{n_2 I_{0L}}{n_L c_0\varepsilon_0}$ and

$$\gamma = (\frac{4n_2 I_{0L}}{n_L c_0\varepsilon_0\tilde{n}})^{1/2}\frac{1}{w} = (\frac{8n_2P}{n_L c_0\varepsilon_0\tilde{n}\pi})^{1/2}\frac{1}{w^2}$$

The laser power is $P = \pi w^2 I_{0L}/2$. Since the Kerr lensing for the Brewster plate in the sagittal and tangential plane is different, the *w* and I_{0L} in (6) equation are replaced by $w \to w_t = n_L w$, $w \to w_s = w$, and $I_{0L} \to I_{0L}w^2/(w_t w_s) = I_{0L}/n_L$. The equations for the sagittal plane of a Brewster plate are given by $n_s = \tilde{n}_B(1-\frac{1}{2}\gamma_s^2 r^2)$ where $\tilde{n}_B = n_L + \frac{n_2 I_{0L}}{n_L^2 c_0\varepsilon_0}$ and

$$\gamma_s = (\frac{4n_2 I_{0L}}{n_L^2 c_0\varepsilon_0\tilde{n}_B})^{1/2}\frac{1}{w} = (\frac{8n_2P}{n_L^2 c_0\varepsilon_0\tilde{n}_B\pi})^{1/2}\frac{1}{w^2} \tag{7}$$

For the tangential plane of a Brewster plate the equation are written as

$$n_t = \tilde{n}_B(1-\frac{1}{2}\gamma_t^2 r^2)$$

with $\gamma_t = (\frac{4n_2 I_{0L}}{n_L^4 c_0 \varepsilon_0 \tilde{n}_B})^{1/2} \frac{1}{w} = (\frac{8n_2 P}{n_L^4 c_0 \varepsilon_0 \tilde{n}_B \pi})^{1/2} \frac{1}{w^2}$ (8)

The Kerr-lens ABCD matrices in the tangential and sagittal plane are given in Table I.

(a) (b)

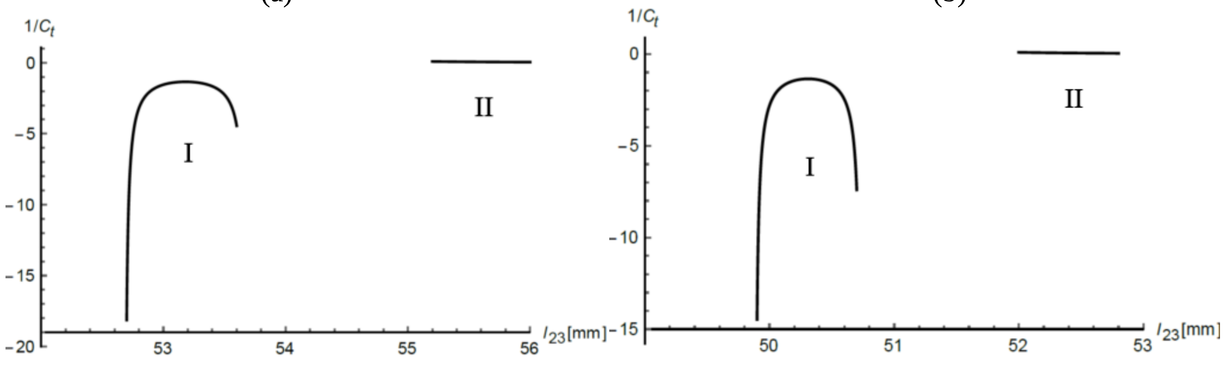

Figure.2 The misalignment sensitivity parameter of the folded-cavity four-mirror resonator without the Kerr lensing (P=0). a.) sagittal plane, b.) tangential plane.

(a) (b)

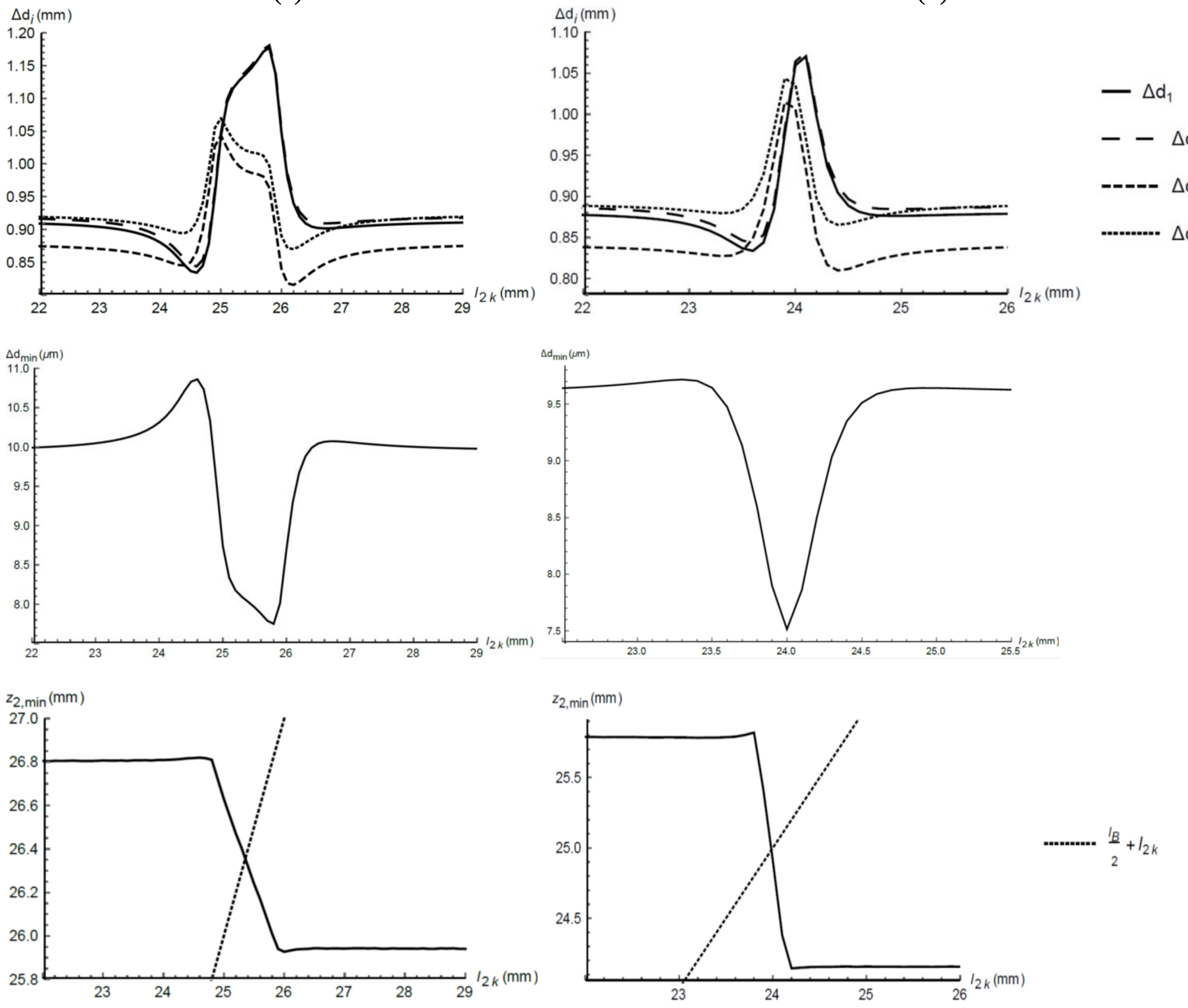

Figure.3 The influence of the Kerr lens position l_{2k} position on beam parameters. Laser power, $P = 2 \times 10^5 W$. Parameters listed in Table II are applied. a.) sagittal plane, b.) tangential plane.

III. SIMULATIONS

There are two stability regions observed in the tangential and sagittal plane of the four-mirror cavity with the astigmatism compensated. Due to the folded mirror separation l_{23} it is divided into two stability zones I and II as shown in the misalignment sensitivity parameter plot (Fig.2) without the Kerr lensing.

In the case with the Kerr lensing the parameter l_{23} is fixed and the Kerr lens position l_{2k} only in the folded cavity is varied. In Fig.3 the beam parameters modifications caused by the Kerr lensing are compared in the tangential and sagittal plane, respectively. The applied resonator parameters are listed in Table II. The plots, shown in Fig.3 corresponds to the beam diameters at the mirrors, the minimum beam diameters in the gain cavity and the position of the beam waist $Z_{2,min}$ measured from the mirror M_2 against the Kerr lens position l_{2k}. The laser power inside the resonator is set to $P = 2\times10^5$ W.

From the beam waist position plots, one can see that by increasing the distance from the M_2 to the crystal (for $l_{2k}>z_{2,min}$), the beam waist exists outside of the crystal, then its position remains constant. It is same for $l_{2k}<z_{2,min}-l_B$ and it shows the lensing effect getting small. When the beam waist exists inside the crystal ($l_{2k}<z_{2,min}< l_{2k} +l_B$), its position decreases until the end of the crystal because of the increase of the beam intensity inside the crystal. Since the beam intensity is high at the face of the crystal, around $l_{2k}=z_{2,min}-l_B$ and $l_{2k}=z_{2,min}$ the Kerr-lens effect is largest.

The beam size is changed in the Brewster plate, causing beam narrowing at some mirrors and beam broadening at others as shown in the plots with the beam diameters dw_i (Fig.3). An aperture setting in regions of beam narrowing leads to Kerr-lens mode locking.

IV. CONCLUSION

We introduced the beam parameters modifications caused by the Kerr lensing in the four-mirror folded-cavity resonator. In the simulation the real parameters of a femtosecond Ti:sapphire laser are used. The astigmatism due to the beam propagation in the sagittal and tangential plane of the folded-cavity is compensated.

The optimum resonator design parameters (slit positioning, gain cavity spacing, and gain medium position) are obtained for maximum Kerr-lens mode-locking effect.

ACKNOWLEDGEMENTS

This work is supported by the fundamental research project No.2019/05, financed by the Mongolian Foundation for Science and Technology.

REFERENCES

[1] Orazio Svelto (2010) *Principles of Lasers*, New York, Springer.

[2] Vittorio Magni, Giulio Cerullo (1993) ABCD matrix analysis of propagation of gaussian beams through Kerr media, Opt Comm 96: 348-355.

[3] A. Penzkofer A, M. Wittmann (1996) Kerr lens effects in a folded-cavity four-mirror linear resonator, Optical and Quantum Electronics 28: 423-442.

[4] D.E Spence, P.N. Kean (1991) 60-fsec pulse generation from a self-mode-locked Ti:sapphire laser, Opt. Lett 16: 42.

[5] A. Malakzadeh, M. Javad Kamjoo, (2017) Simulation of Kerr lens modelocking behaviour in sagittal plane, Laser Opt Photonics 4:1.

[6] S. Chen, J. Wang(1991) Self-starting issues of passive self-focusing mode-locking. Opt Lett 16: 1689-1691.

[7] P. Curley, A. Ferguson (1991) Actively mode-locked Ti: sapphire laser producing transform-limited pulses of 150-fs duration, Opt. Lett 16: 1016-1018.

[8] D.E Spence, J Evans (1991) Regeneratively initiated selfmode-locked Ti: sapphire laser, Opt Lett 16: 1762-1764.

[9] N. Sarukura, Y. Ishida (1991) Generation of 50-fsec pulses from a pulse-compressed, CW, passively mode-locked Ti: sapphire laser, Opt Lett 16: 153-155.

[10] P. French, S Kelly (1989) Femtosecond pulse generation from a titanium-doped sapphire laser using nonlinear external cavity feedback, Opt. Lett 14: 686-688.

[11] P. French, D. Noske (1991) Characterization of a cw titanium-doped sapphire laser mode-

locked with a linear external cavity, Opt Comm 83: 185-194.

[12] W. Pelouch, P. Powers, C. Tang (1992) Ti: sapphire-pumped, high-repetition-rate femtosecond optical parametric oscillator, Opt Lett 17: 1070-1072.

[13] Y.M. Liu , K.W. Sun, P. Prucnal (1992) Simple method to start and maintain self-mode-locking of a Ti: sapphire laser, Opt Lett 17: 1219-1221.

[14] U. Emmerichs, H. Bakker, H. Kurz (1994) Generation of high-repetition rate femtosecond pulses tunable in the mid-infrared, Opt Comm 111: 497-501.

[15] C. Radzewicz, G.W. Pearson, J.S. Krasinski (1993) Use of ZnS as an additional highly nonlinear intracavity self-focusing element in a Ti: sapphire selfmodelocked laser, Opt Comm 102: 464-468.

[16] M.T. Asaki, C.P. Huang (1993) Generation of 11-fs pulses from a self-mode-locked Ti:sapphire laser, Opt Lett 18: 977-979.

[17] J. Kafka, M. Watts, J Pieterse (1992) Picosecond and femtosecond pulse generation in a regeneratively mode-locked Ti: sapphire laser, Optical and Quantum Electronics IEEE 28: 2151-2162.

[18] R. L. Fork, E. Martinez, and J. P. Gordon (1984) Negative dispersion using pairs of prisms, Opt. Lett. 9: 150-152.

[19] Xinglong Wang, Guojiang Hu (1994) Numerical analysis of beam parameters and stability regions in a folded or ring cavity, J. Opt. Soc. Am. A 11: 8.

[20] H. Kogelnik, (1996) T. Li, Appl. Opt. 13: 1550

[21] R. E. Sherri (1998) Analytic expressions for group-delay dispersion and cubic dispersion in arbitrary prism sequences, J. Opt. Soc. Am. B 15: 1224-1230.

[22] H. A. Haus, (2000) Mode-locking of lasers, IEEE J. Sel. Topics Quantum Electron. 6: 1173-1185.

[23] B. Meier, A. Penzkofer (1989), Appl. Phys. B 49: 513.

[24] Ts. Baatarchuluun, Byeong Kwan Yang, (2007) A sub-10-fs Ti:sapphire oscillator with a simple four-mirror cavity, J. Korean Phys. Soc Vol 52, 4: 1043-104.